

# Oceanalin A, a Hybrid $\alpha,\omega$ -Bifunctionalized Sphingoid Tetrahydroisoquinoline $\beta$ -Glycoside from the Marine Sponge *Oceanapia* sp.

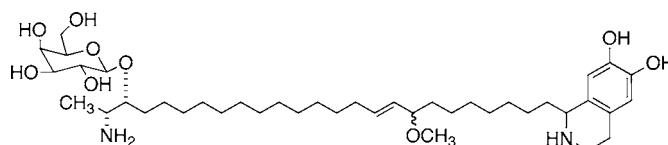
Tatyana N. Makarieva,<sup>†</sup> Vladimir A. Denisenko,<sup>†</sup> Pavel S. Dmitrenok,<sup>†</sup>  
Alla G. Guzii,<sup>†</sup> Elena A. Santalova,<sup>†</sup> Valentin A. Stonik,<sup>†</sup> John B. MacMillan,<sup>‡</sup> and  
Tadeusz F. Molinski<sup>\*,‡</sup>

Department of Chemistry, University of California–Davis, Davis, California 95616,  
and Laboratory of MaNaPro Chemistry, Pacific Institute of Bioorganic Chemistry of  
the Russian Academy of Sciences, 690022 Vladivostok, Russia

tfmolinski@ucdavis.edu

Received April 12, 2005

## ABSTRACT



The novel antifungal compound oceanalin A, an unprecedented “hybrid sphingolipid”, was isolated from the marine sponge *Oceanapia* sp. The structure was elucidated using NMR and MS spectral analysis and chemical degradation. Oceanalin A exhibits in vitro antifungal activity against *Candida glabrata* with an MIC of 30  $\mu\text{g/mL}$ .

Long-chain sphingolipids and sphingoid bases exhibit antifungal activity against the pathogenic fungus, *Candida glabrata*.<sup>1</sup> In our continuing investigation of antifungal dimeric sphingolipids with novel modes of activity, we analyzed several marine invertebrate extracts for the presence of long-chain dimeric sphingoid bases. We report here the structure elucidation of an unprecedented tetrahydroquinoline-containing dimeric sphingolipid, oceanalin A (**1**), along with the known rhizochalin (**2**), from an ethanolic extract of the marine sponge *Oceanapia* sp., collected off the northwest coast of Australia.<sup>2</sup> The new compound **1** has an unexpected structure with different polar termini that conforms to a

hypothesis<sup>2b</sup> that **1**, **2**, and other dimeric sphingolipids derive from modular biosynthesis involving long-chain ketide extensions coupled with terminal functionalization by *independent* biosynthetic pathways.

Compound **1** is antifungal against the human pathogen *Candida glabrata* (MIC 30  $\mu\text{g/mL}$ ) and appears to block sphingolipid biosynthesis by inhibiting ceramide synthase.<sup>3</sup> The biosynthesis of one terminus in **1** resembles that of the phytotoxic fumonisins B<sub>1</sub>, a sphingoid long-chain base from *Fusarium* spp. that derives from L-alanine,<sup>4</sup> while the other terminus is a 1-substituted tetrahydroisoquinoline similar to those found in higher plants.<sup>5</sup> Oceanalin A joins a unique group of bifunctionalized sphingolipids, including **2** and

<sup>†</sup> Pacific Institute of Bioorganic Chemistry of the Russian Academy of Sciences.

<sup>‡</sup> University of California–Davis.

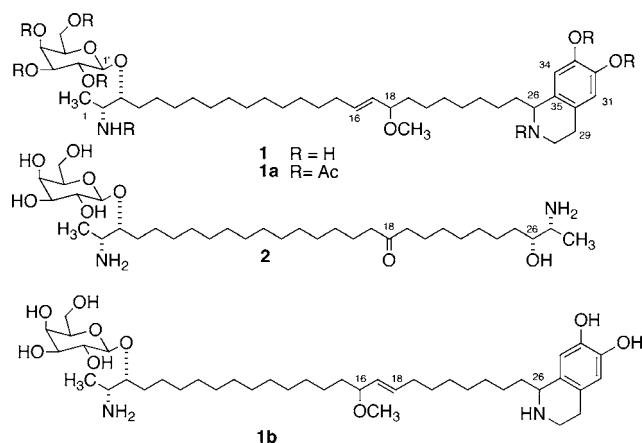
(1) (a) Richter, R. K.; Mickus, D. E.; Rychnovsky, S. D.; Molinski, T. F. *Bioorg. Med. Chem. Lett.* **2004**, *14* (1), 115–118. (b) Molinski, T. F. *Curr. Med. Chem.: Anti-Infect. Agents* **2004**, *3*, 197–220.

(2) (a) Makarieva, T. N.; Denisenko, V. A.; Stonik, V. A.; Milgrom, Yu. N.; Rashkes, Ya. W. *Tetrahedron Lett.* **1989**, *30*, 6581–6584. (b) Molinski, T. F.; Makarieva, T. N.; Stonik, V. A. *Angew. Chem., Int. Ed.* **2000**, *39*, 4076–4079.

(3) Dalisay, D. S.; Molinski, T. F. Unpublished results. Presented in part at the *1st International Symposium on Marine Drugs*; Qingdao, PR China, October 18–22, 2004.

(4) (a) Blackwell, B. A.; Edwards, O. E.; Fruchier, A.; ApSimon, J. W.; Miller, J. D. In *Fumonisin in Food*; Jackson, L., Ed.; Plenum Press: New York, 1996. (b) Boyle, C. D.; Harmange, J.-C.; Kishi, Y. *J. Am. Chem. Soc.* **1994**, *116*, 4995–4996. (c) Branham, B. E.; Plattner, R. D. *Mycopathologia* **1993**, *124*, 99–104.

oceanapiside,<sup>6</sup> that differ substantially from mammalian long-chain bases (e.g., D-sphingosine) and exhibit potent antifungal activity against the Fluconazole-resistant pathogen, *C. glabrata*.<sup>1,6</sup> In this report, we describe the isolation and structure elucidation and antifungal activity of **1**.



The EtOH extract of the lyophilized sponge was concentrated and partitioned between aqueous EtOH and hexane. The aqueous EtOH layer was further partitioned against *n*-BuOH, and the *n*-BuOH-soluble materials were separated by ODS flash chromatography and repeated reversed-phase HPLC to give oceanalin A (**1**) as a colorless amorphous solid (0.003% dry weight;  $[\alpha]_D -5.7^\circ$  (c 0.14 EtOH)) that tested positive for a free primary amino group (ninhydrin). The molecular formula of oceanalin A (**1**) was established as  $C_{41}H_{72}N_2O_9$  on the basis of NMR and HRFABMS data ( $m/z$  737.5286,  $MH^+$ , calcd 737. 5311  $C_{41}H_{73}N_2O_9$ ).

A doubly protonated molecular ion ( $m/z$  369, 30%,  $[M + 2H]^{2+}$ ) dominates the ESI mass spectrum of **1**, as is characteristic of bifunctionalized sphingolipids.<sup>2a,6a</sup> Initial analysis of NMR data (Table 1) showed signals for the presence of a hexose residue (anomeric carbon  $\delta_H$  4.32 d,  $J = 7.2$  Hz;  $\delta_C$  104.8), a tetrasubstituted aromatic ring, a nitrogen-substituted  $CH_2$  ( $\delta_H$  3.30 and 3.50;  $\delta_C$  41.6), two N-substituted CH carbons ( $\delta_H$  4.32 and 3.17;  $\delta_C$  57.3 and 52.7), two oxygenated methines ( $\delta_H$  3.68 and 3.50;  $\delta_C$  80.9 and 84.7), a disubstituted double bond ( $\delta_H$  5.20 and 5.63;  $\delta_C$  132.2 and 136.6), a secondary methyl ( $\delta_H$  1.25;  $\delta_C$  16.0), and one OMe group ( $\delta_H$  3.20;  $\delta_C$  56.6) (Table 1). The remainder of the  $^1H$  NMR signals for **1** could be attributed to long methylene chains ( $\delta_H$  1.20–1.30, m). Peracetylation of **1** ( $Ac_2O$ , pyridine) gave the octaacetyl derivative **1a**, which supports the presence of six OH groups and two amines, a primary  $NH_2$  and a secondary  $NH$ .

Interpretation of two-dimensional NMR data provided substructures **a–c** (Figure 1). Substructure **a** contains one hexopyranose residue attached by a  $\beta$ -O-glycosidic bond ( $\delta_H$

**Table 1.**  $^1H$  and  $^{13}C$  NMR Data for Oceanalin A (**1**)<sup>a</sup>

	$\delta_C$	$\delta_H$ (mult, $J$ Hz)	COSY	gHMBC <sup>b</sup>
1	16.0	1.28 (d, 6.7)	H2	H26
2	52.7	3.17 (m)	H1, H3	H1, H2
3	80.9	3.68 (ddd, 3.2, 7.2, 9.7)	H2, H4a, H4b	H1, H2, H1'
4a	33.3	1.52 (m)	H3	
4b		1.68 (m)	H3	
5				
6–13	30.8–31.6	1.27–1.29 (bs)		
14	31.0	1.45 (m)		
15	33.9	2.06 (m)	H16	H16, H17
16	136.6	5.63 (dt, 15.0, 7.2)	H17, H15	H15, H14, H18
17	132.2	5.20 (dd, 8.3, 15.0)	H16, H18	H15
18	84.7	3.50 (m)	H17, H19a, H19b	OMe, H16
19a	37.3	1.55	H18	
19b		1.40	H18	
20–24	30.8–31.6	1.27–1.29		
25	35.7	2.00 (m), 1.88 (m)	H26	H26
26	57.3	4.32 (dd, 4.3, 8.0)	H25a, H25b	H34, H25, H28
2-NHAc				
28a	41.6	3.30 (m)	H29a, H29b	H29a, H29b, H26
28b		3.50 (m)	H29a, H29b	
29a	27.0	2.89 (dt, 17.0, 6.0)		H28a, H28b, H31
29b		2.97 (ddd, 5.7, 7.7, 17.0)		
30	124.2			H29, H28, H34
31	116.8	6.60 (s)		H29a, H29b
32	147.3			H34
33	146.5			H31
34	114.5	6.64 (s)		
35	124.8			H25, H26, H31
OMe <sub>3</sub>	56.6	3.20		
1'	104.6	4.32 (d, 7.2)	H2'	H3, H2'
2'	73.3	3.51 (dd, 7.2, 9.8)	H3', H1'	H3', H4'
3'	75.1	3.47 (dd, 3.4, 9.8)		
4'	71.1	3.78 (d, 3.4)		
5'	77.6	3.54 (dd, 4.6, 6.5)		H6', H5'
6'	63.6	3.72 (m) <sup>c</sup> , 3.74 (m) <sup>c</sup>		

<sup>a</sup>  $CD_3OD$ , 500 MHz. <sup>b</sup> Performed at 600 MHz. <sup>c</sup> AB part of the ABX spin system:  $J_{gem} = -11.8$  Hz;  $J_{vic} = 4.6, 7.5$  Hz.

4.32, d,  $J = 7.2$  Hz, H1') to a 2-amino-3-alkanol fragment. Characteristic NMR chemical shifts of the anomeric  $^1H$  signal H-1' and the C-3  $^{13}C$  signal ( $\delta_C$  80.9), together with a  $^3J$   $^1H$ – $^{13}C$  correlations between these two signals, confirmed

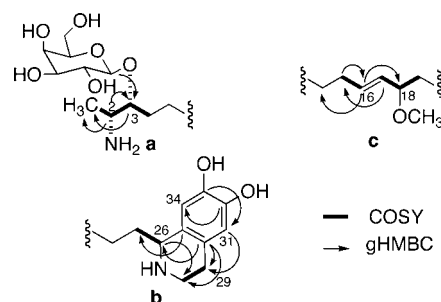


**Figure 1.** Partial structures of **1** with selected HMBC correlations.

(5) Conn, E. E. In *The Biochemistry of Plants: A Comprehensive Treatise*; Stumpf, P. K., Conn, E. E., Eds.; Academic Press: New York, 1980; Vol. 7.

(6) (a) Nicholas, G. M.; Hong, T. W.; Molinski, T. F.; Lerch, M. L.; Cancilla, M. T.; Lebrilla, C. B. *J. Nat. Prod.* **1999**, 62, 1678–1681. (b) Nicholas, G. M.; Molinski, T. F. *J. Am. Chem. Soc.* **2000**, 122, 4011–4019.

the location of the hexose at C-3. Complete assignments of the remaining  $^1\text{H}$  and  $^{13}\text{C}$  NMR signals were based on COSY and gHMBC data.

Substructure **b** was composed of two proton spin systems. Interpretation of the COSY data starting from the H-25 methylene protons ( $\delta$  2.00, m; 1.88, m) led to a deshielded proton at H-26 ( $\delta$  4.32, dd,  $J$  = 8.0, 4.3 Hz, 1H), flanking an N atom that was further connected to a second spin system comprised of an ethylene group, H<sub>2</sub>-28 ( $\delta$  3.30 m; 3.50, m) and H<sub>2</sub>-29 ( $\delta$  2.89, dt,  $J$  = 17.0, 6.0 Hz; 2.97, ddd,  $J$  = 17.0, 7.7, 5.7 Hz), positioned between the N atom and an aromatic ring, which was readily inferred from the  $^1\text{H}$  and  $^{13}\text{C}$  NMR chemical shift values (Table 1). The  $^{13}\text{C}$  NMR chemical shift values for C-32 ( $\delta$  147.3) and C-33 ( $\delta$  146.5) were consistent with a catechol.

Integrated analysis of the UV absorption spectrum [ $\lambda$  238 ( $\epsilon$  7600), 288 nm ( $\epsilon$  7850)],<sup>7</sup> the chemical shifts of the aryl proton signals H-31 ( $\delta_{\text{H}}$  6.60, s) and H-34 ( $\delta_{\text{H}}$  6.64, s), and two-dimensional NMR cross-peaks present in the HMBC spectrum (C-31/H-29, C-30/H-29, H-28, H-26, H-34 and C-26/H-28) revealed the second terminus to be a 1,6,7-trisubstituted tetrahydroisoquinoline (substructure **b**). Additional HMBC cross-peaks (e.g., C-32/H-34, C-33/H-31, C-35/H-25) were fully supportive of the substructure **b**.

Substructure **c** consists of an allylic *O*-methyl ether unit flanked by polymethylene chains. HMBC cross-peaks C-16/H-14 and C-16/H-18, C-17/H-15, C-15/H-16 confirmed placement of the OMe group at the allylic position. COSY cross-peaks were observed for a consecutive spin sequence starting from the allylic CH<sub>2</sub> protons H<sub>2</sub>-15 ( $\delta$  2.06, m, 2H) to H-16 ( $\delta$  5.63, dt,  $J$  = 7.2, 15 Hz), to H-17 ( $\delta$  5.20, dd,  $J$  = 8.3, 15 Hz), an *O*-substituted CH, H-18 ( $\delta$  3.50, m, 1H), and finally connecting to the diastereotopic H-19 CH<sub>2</sub> group ( $\delta$  1.55, m; 1.40, m). The olefinic  $^1\text{H}$  vicinal coupling constant ( $J$  = 15 Hz) and  $^{13}\text{C}$  chemical shift of the allylic methylene C-15 ( $\delta$  33.9)<sup>8</sup> were consistent with an (*E*)-double bond.

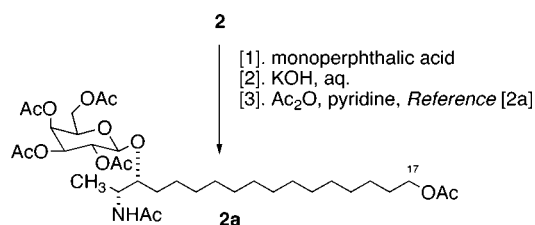


**Figure 2.** Oxidative degradation of **2**.

Initial attempts to position the CH=CH-CH(OMe) group in **1** by mass spectrometry were unsuccessful, as neither the FABMS nor MALDI spectra of **1** showed  $\alpha$  or  $\beta$  cleavage fragment ions. The EIMS spectrum of the peracetate **1a**

showed only multiple losses of ketene and CH<sub>3</sub>COOH. A successful solution to the problem was achieved as follows. The peracetate **1a** was subjected to reductive ozonolysis (O<sub>3</sub>, then NaBH<sub>4</sub>) followed by acetylation (Ac<sub>2</sub>O, pyridine). The two main products isolated by HPLC of the crude mixture were peracetates **3** and **4** (Figure 3), along with the

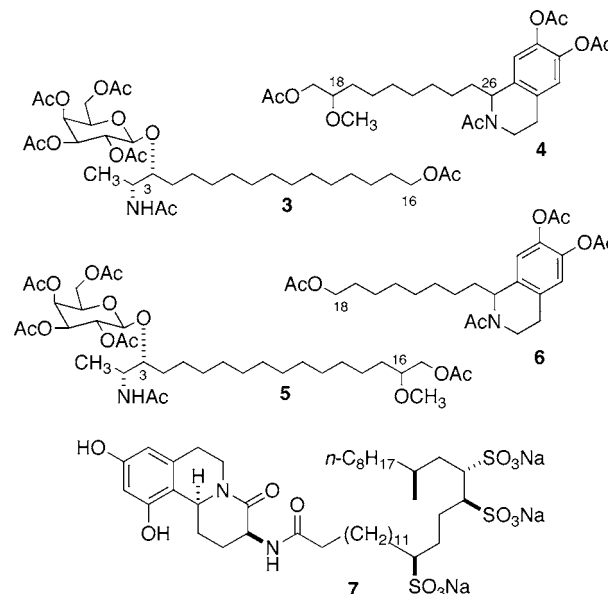


**Figure 3.** Structures of degradation products and schulzeine A (**7**).<sup>14</sup>

corresponding isomers **5** and **6** (combined, 20%; see Supporting Information), the latter presumably arising from the rearranged isomer **1b**.<sup>9</sup> NMR data confirmed that compound **3** retained the glycosylated terminus, while the derivative **4** was a tetrahydroisoquinoline substituted chain, terminated by an *O*-acetoxy-glycol unit. Pseudomolecular ions [ $M + \text{Na}$ ]<sup>+</sup> observed at  $m/z$  710 and 528 in the MALDI-TOF MS for compounds **3** and **4**, respectively, permitted us to locate the position of the allylic ether as shown in **1**.

The absolute configuration of **1** was addressed as follows. Hydrolysis of **1** (6 N HCl, 100 °C, 2.5 h) gave D-galactose. The ozonolysis product **3** obtained from **1a** was indistinguishable (NMR,  $[\alpha]_{\text{D}}$ ) from the known homologue **2a** obtained previously by a different oxidative degradation of rhizochalin (**2**).<sup>2a</sup> Since the absolute configuration of **2** was established by interpretation of CD spectra of tetra-*N,O*-benzoyl derivatives obtained from **2**, oceanalin A (**1**) has

(9) Products **5** and **6** were isolated as peracetates from the ozonolysis–reduction of a minor regioisomer **1b** that is present as an inseparable impurity in **1** (~20%). NMR data confirmed that compound **5** retained the galactose-containing moiety and CH(OMe) fragments, while the derivative **6** contained the tetrahydroisoquinoline unit. Observation of pseudomolecular ions [ $M + \text{Na}$ ]<sup>+</sup> observed at  $m/z$  754 and 484 in MALDI-TOF spectra of **5** and **6** confirmed their identities. Compound **1b** appears to have originated from an acid-catalyzed allylic rearrangement of the allylic *O*-Me ether in **1**, possibly during its isolation by HPLC (0.1% TFA MeOH/H<sub>2</sub>O). Since this central substructure is essentially “insulated” from the terminal functional groups by long CH<sub>2</sub> chains, the regioisomerism was not perceptible in the  $^1\text{H}$  NMR spectra of the mixture **1/1b**, even at 600 MHz.

(7) Kohimoto, S.; McConnell, O. J.; Wright, A. *Experientia* **1988**, *44*, 85–86.

(8) Choudhury, S. R.; Traquair, J. P.; Jarvis, W. R. *Can. J. Chem.* **1995**, *73*, 84–87.

the same (2*R*,3*R*)-configuration as rhizochalin.<sup>2</sup> Compounds **1**, **1a**, **4**, and **6** showed only weak optical rotations ( $[\alpha]_D$  0~1°) and an absence of a benzenoid Cotton effect in the CD spectrum at the wavelength expected for 1-substituted 6,7-dihydroxy-tetrahydroquinolines ( $\lambda$  270 nm).<sup>10</sup> Given that the latter compounds show a propensity for spontaneous epimerization at C-1 (isoquinoline numbering),<sup>11</sup> we conclude that **6** is racemic and that **1** and **1a** exist as 1:1 mixtures of C-26 epimers.<sup>12</sup>

Doubling was observed for <sup>1</sup>H NMR signals of the 32,33-*O*- and *N*-acetyl groups, and nearby signals of peracetates **1a**, **4**, and **6** containing a tetrahydroisoquinoline group (Table 1). This was attributed to slow rotation about the tertiary acetamide (*N*-27-Ac) and is a well-known property of the NMR spectra of *N*-acetyltetrahydroisoquinolines.<sup>13</sup> At elevated temperature (*T* = 80 °C), the doubled acetyl signals in <sup>1</sup>H NMR spectrum of **4** (*d*<sub>5</sub>-pyridine) collapsed into a single set of discrete singlets (see Supporting Information for detailed temperature-dependent <sup>1</sup>H NMR data for **4**).

Isoquinolines are rare among marine natural products. The schulzeines (e.g., schulzeine A, **7**) are a new family of tetrahydroisoquinolines, recently isolated from the marine sponge *Penares schulzei*,<sup>14</sup> and like oceanalin A (**1**) contain a dihydroxytetrahydroisoquinoline fragment but differ in the positions of the phenoxyl groups. The heterocyclic rings of **1** and **7** are substituted at C-1 (isoquinoline numbering) with a long alkyl chain, but unlike **1**, the schulzeines lack functionalization at the  $\omega$ -terminus. Most naturally occurring 6,7-dihydroxy 1-substituted tetrahydroquinolines are derived from condensation of tyramine, phenylethylamine, or dopamine with simple aldehydes or  $\alpha$ -ketocarboxylic acids, with concomitant decarboxylation.<sup>15</sup>

The bifunctionalized sphingolipids **1**, **2**,<sup>2</sup> calyxoside,<sup>16</sup> and oceanapiside<sup>5</sup> all possess a conserved number of carbon atoms (C<sub>24</sub>) in the long chains between the functionalized termini, which suggests that they derive from similar lipid carboxyl precursors.<sup>17</sup> The biosynthesis of the sphingolipid  $\alpha$ -terminus in **1** and **2** most likely proceeds by pyridoxal

phosphate-dependent condensation of alanine with a fatty acyl CoA ester, as shown for fumonisins B<sub>1</sub> by labeling studies.<sup>4c</sup> The former sequence is also likely for the biosynthesis of shorter chain C<sub>12</sub>–C<sub>18</sub> marine-derived 2-amino-3-alkanol sphingoid bases.<sup>18</sup>

A remarkable corollary that arises from consideration of the structures of **1** and **2** is that their biosynthesis adopts “modular-ketide tailoring” reactions to elaborate differently functionalized  $\alpha$ - and  $\omega$ -termini.<sup>5a</sup> In the case of **1**, this hybrid biogenesis leads to a remarkable confluence of sphingolipid and isoquinoline pathways in natural products biosynthesis.

Oceanalin A (**1**) showed antifungal activity against the Fluconazole-resistant yeast *C. glabrata* with a minimum inhibitory concentration (MIC) of 30  $\mu$ g/mL in broth dilution experiments, which is comparable to the activity of D-sphingosine (MIC 30  $\mu$ g/mL).<sup>1a</sup> Preliminary studies show that **1** blocks phytosphingolipid biosynthesis in *C. glabrata*.<sup>3</sup> Studies are underway in our laboratory to refine our understanding of the mechanism of action of **1**.

**Acknowledgment.** The authors kindly acknowledge Mr. V. B. Krasokhin for identification of the sponge. We also thank Miss K. N. Yu for measurements of CD spectra, R. Kondrat (UC Riverside) for FABMS measurements, and Doralyn Dalisay for some fungal susceptibility measurements. This investigation was supported by the Fogarty International Center and NIH (RO3 TWO06301 and RO1 AI39887 to T.F.M) and, in part, by the Program of Presidium of RAS “Molecular and Cell Biology” Grant N04-1-05-005, Grant N SS-725.2003.4 from the President of RF, and Grant FEB RAS N 04-3-G-05-055.

**Supporting Information Available:** General procedures for isolation of **1**, <sup>1</sup>H and <sup>13</sup>C NMR, DEPT, COSY, HSQC, HMBC (*J* = 8 Hz) of **1**, procedures for degradation of **1**, and <sup>1</sup>H NMR, MS, and  $[\alpha]_D$  data for peracetates **3**–**6**. This material is available free of charge via the Internet at <http://pubs.acs.org>.

OL050796C

(10) (a) Snatzke, G. *Angew. Chem., Int. Ed. Engl.* **1979**, *18*, 363–377. (b) Rozwadowska, M. D.; Brossi, A. *J. Org. Chem.* **1989**, *54*, 3202–3205.

(11) Chrisey, L. A.; Brossi, A. *Heterocycles* **1990**, *30*, 267–270.

(12) Configuration of C-18 was not defined.

(13) (a) De Koning, C. B.; Van Otterlo, W. A. L.; Michael, J. P. *Tetrahedron* **2003**, *59*, 8337–8345. (b) Kitamura, M.; Tsukamoto, M.; Takaya, H.; Noyori, R. *Bull. Chem. Soc. Jpn.* **1996**, *69*, 1695–1700. (c) Fraenkel, G.; Cava, M. P.; Dalton, D. R. *J. Am. Chem. Soc.* **1967**, *89*, 329–332.

(14) Takada, K.; Uehara, T.; Nakao, Y.; Matsunaga, S.; Van Soest, R. W. M.; Fusetani, N. *J. Am. Chem. Soc.* **2004**, *126*, 187–193.

(15) (a) Battersby, A. R.; Binks, R.; Huxtable, R. *Tetrahedron Lett.* **1968**, *9*, 6111–6115. (b) Lundström, J. In *The Alkaloids*; Brossi, A., Ed.; New York, 1983; Vol. 21, p 312.

(16) Zhou, B. N.; Mattern, M. P.; Johnson, R. K.; Kingston, D. G. I. *Tetrahedron* **2001**, *57*, 9549–9554.

(17) A reasonable hypothesis for the origin of the heterocyclic ring in **1** and **7** is condensation of a long-chain dialdehyde or a bifunctionalized  $\alpha$ -keto acid precursor (keto group corresponding to C-26) with dopamine followed by Pictet–Spengler-type intramolecular electrophilic substitution at C-35 to close the tetrahydroisoquinoline ring.

(18) Members of the family of naturally occurring C<sub>12</sub>–C<sub>18</sub> 2-amino-3-alkanols display considerable stereochemical heterogeneity, with the (2*R*,3*S*)-configuration being the most common configuration. (a) Kossuga, M. H.; MacMillan, J. B.; Rogers, E. W.; Molinski, T. F.; Nascimento, G. S. F.; Rocha, R. M.; Berlinck, R. G. S. *J. Nat. Prod.* **2004**, *67*, 1879–1881. (b) Clark, R. J.; Garson, M. J.; Hooper, J. N. A. *J. Nat. Prod.* **2001**, *64*, 1568–1571. (c) Gulavita, N. K.; Scheuer, P. J. *J. Org. Chem.* **1989**, *54*, 366–369. (d) Mori, K.; Matsuda, H. *Liebigs Ann. Chem.* **1992**, 131–137. (e) Cuadros, R.; Montego de Garcini, E.; Wandosell, F.; Faircloth, G.; Fernández-Suárez, J. M.; Avila, J. *Cancer Lett.* **2000**, *152*, 23–29.